GSA DATA REPOSITORY 2019354

Diagenesis Affects the Carbon Isotope Value of Fossil Wood

William E. Lukens, Peace Eze, and Brian A. Schubert*
Correspondence to: william.lukens@louisiana.edu

Site Descriptions and Sample Ages

The wood fossils analyzed in this study were recovered from 4 localities. Geologic descriptions and age control are given as follows.

Banks Island, Arctic Canada (Early Eocene)

Wood samples were collected from the Cyclic Member of the Eureka Sound Formation at the Eames River site on northern Banks Island, Northwest Territories (~74^{o} N) (Padilla et al., 2014; Schubert et al., 2012). The site is dated to early Eocene in age based on palynology, including the presence of Platycarya, rare fossil turtle shell fragments identified as Emydidae (pond turtles, collected by Jaelyn Eberle in 2004), and sharks' teeth referred to the genus Physogaleus (Carcharhinidae) collected from marine sediments. Sharks' teeth referred to Striatolamia (Odontaspididae; sand tigers), which have a Paleocene-Eocene distribution, are also known from the site (Padilla et al., 2014). Wood fossils from the nearby Muskox River site were previously described in Schubert et al. (2012).

Nanning, China (Oligocene)

Fossil wood samples were collected from the Yongning Formation of the south China Nanning Basin (22.881° N, 108.417° E). The wood is part of a Konservat-Lagerstätte that preserves tree trunks, branches, roots, leaves, fruiting bodies, seeds, and fungi, as well as invertebrate and vertebrate fossils (Huang et al., 2018; Quan et al., 2016; Ying et al., 2018). The age for the site is assigned based on anthracotheriid mammals and a late Oligocene tragulid (Zhao, 1993). The fossil wood is preserved in a single, fining-upward deposit that occurs between deepwater lacustrine mudstones (Quan et al., 2016). Rounded gravels and the dense accumulation of fossils indicate that the Lagerstätte was rapidly deposited in a single event. Palynology of the lacustrine mudstones and the wood-bearing interval indicates a conifer-dominated, temperate forest surrounded the lake basin (Ying et al., 2018).

Yunnan, China (late Miocene)

Wood fossils were collected from the Xiaolongtan Formation (25.416° N, 102.850° E) in the Yunnan Province, China (Xing et al., 2010). The Xiaolongtan Formation consists of interbedded coal, lignite, mudstone, siltstone, and diatomite. A late Miocene age was determined based on mammalian fauna (Dong, 2001; Zhang, 1974) and floral assemblages (Wang et al., 1999; Zhou, 1985; Zhou, 2000).

Finish Stream, Sakha Republic, Russia (late Miocene)

Fossil wood was collected from the Upper Miocene Khapchansky horizon at "Finish Stream" in far northeastern Siberia (present-day coordinates: 68.724° N, 161.587° E;

paleolatitude: 71–72° N (van Hinsbergen et al., 2015), as described within (Schubert et al., 2017). The sediments contain silt lenses and ferruginous sands containing plant detritus and the wood fragments sampled here. A palynological analysis was consistent with the late Miocene age for the site. A lack of thermophilic angiosperm pollen suggests the sediments postdate the Miocene Climate Optimum (17 to 15 Ma); stratigraphic position below the very coarse-grained Lower Pliocene Begunovsky horizon suggests the wood predates the early Pliocene. Details on the Finish Stream locality, stratigraphy, wood fossils, and palynological analysis can be found within (Schubert et al., 2017).

Analytical Methods

Fossil samples were dried overnight at 40-50°C and then ground and homogenized in an agate mortar and pestle. Where growth rings were visible, homogenized samples typically included between 2-5 rings. Powdered whole wood samples were wrapped in tin capsules and stored in a desiccator. Aliquots of the same powders were set aside for cellulose extraction. Cellulose (α-cellulose) was extracted using the Brendel method (Brendel et al., 2000), modified with a NaOH treatment (Gaudinski et al., 2005). The NaOH washing has been shown to prevent addition of C and N to cellulose, and to remove excess residues of lipids and waxes (Gaudinski et al., 2005). Cellulose content was calculated as the difference in sample mass before and after extraction and is reported in weight percent. Cellulose content could not be accurately measured for some samples that contained detrital silicate mineral grains left behind in extracted cellulose, and are reported as "NA" in Table DR2.
The isotopic composition of extracted cellulose and whole wood was analyzed using a Delta V Advantage Isotope Ratio Mass Spectrometer (Thermo Fisher) coupled to a Thermo Finnigan Elemental Analyzer (Flash EA1112 Series, Bremen, Germany) at the University of Louisiana at Lafayette. Three internal lab standards were used for carbon isotope ratio calibration (JGLY, –43.51‰; JHIST, –8.15‰; and JRICE, –27.44‰); a fourth (JGLUC, –10.52‰) was analyzed as an unknown quality assurance sample. Analytical precision of the quality control sample was ± 0.2‰ (± 1σ, n = 10). All isotope ratios are reported relative to the Vienna Pee Dee Belemnite (VPDB) standard: $\delta^{13}C = [(R_{sample}/R_{standard}) – 1] * 1000$, where R is the ratio of ^{13}C to ^{12}C. The internal reference materials were calibrated within our laboratory and normalized to VPDB using NBS-19 calcium carbonate ($\delta^{13}C$ consensus value = 1.95‰) and LSVEC lithium carbonate ($\delta^{13}C$ consensus value = -46.6‰), which define the VPDB scale (Coplen et al., 2006). All isotope ratios are reported relative to the Vienna Pee Dee Belemnite (VPDB) standard: $\delta^{13}C = [(R_{sample}/R_{standard}) – 1] * 1000$, where R is the ratio of ^{13}C to ^{12}C.

Estimation of pCO_2 Using Fossil Wood

We determined pCO_2 at the Toarcian CIE using the following equation that relates changes in net carbon isotope discrimination [$\Delta^{13}C = (\delta^{13}C_{atm} - \delta^{13}C_{wood}) / (1 + \delta^{13}C/1000)$] between two time points (time t and $t = 0$) to changes in pCO_2 (Schubert and Jahren 2015):

$$[(\delta^{13}C_{atm(t)} - \delta^{13}C_{(t)}) / (1 + \delta^{13}C_{(t)}/1000)] - [(\delta^{13}C_{atm(t=0)} - \delta^{13}C_{(t=0)}) / (1 + \delta^{13}C_{(t=0)}/1000)] = [(A)(B)(pCO_{2(t)} + C)] / [(A + (B)(pCO_{2(t)} + C)] - [(A)(B)(pCO_{2(t=0)} + C)] / [(A + (B)(pCO_{2(t=0)} + C)] \quad \text{(Eqn. DR1)}$$

where time t is the peak of the carbon isotope excursion (stratigraphic height between 1780 and 2080 cm; Hesselbo et al., 2007) and time $t = 0$ is the post-industrial Holocene. Within Eqn. (DR1), we set A = 28.26, B = 0.22, and C = 23.9 (Schubert and Jahren, 2015); $\delta^{13}C_{atm(t=0)}$ = -7.6‰ (Keeling et al., 2001) and $\delta^{13}C_{atm(t)}$ = -7.2‰ (using bulk marine carbonate $\delta^{13}C$ from Hesselbo et al., 2007, and assuming a 7‰ offset between the bulk marine carbonate $\delta^{13}C$ value, after Prokoph et al., 2008); $\delta^{13}C_{(t=0)}$ = -24.4‰ (median post-industrial evergreen gymnosperm $\delta^{13}C_{wood}$ value; Table DR2, n = 139); and $pCO_{2(t=0)}$ = 350 ppm (Keeling et al., 2001). When using $\delta^{13}C_{(t)}$ = -29.4‰ (median $\delta^{13}C_{wood}$ at time t, Hesselbo et al., 2007, n = 10), Eqn. (DR1) yields $pCO_{2(t)}$ = 2154 ppm. Although cellulose content was not measured in these samples, trends observed in our Cenozoic dataset suggest that cellulose content was likely low (i.e., < 1%) in these Mesozoic samples, suggesting an inherent bias of ~1.4‰ compared to background modern $\delta^{13}C_{wood}$ values. Adjusting $\delta^{13}C_{(t)}$ by 1.4‰ (i.e., $\delta^{13}C_{(t)}$ = -28.0‰ versus -29.4‰) to account for this cellulose loss yields $pCO_{2(t)}$ = 1039 ppm (Eqn. DR1), or 1115 ppm lower than $pCO_{2(t)}$ calculated without accounting for diagenesis (i.e., 2154 ppm). We note that this corrected $pCO_{2(t)}$ estimate (i.e., 1039 ppm) overlaps with an estimate of 1200 ± 400 ppm based on fossil leaf stomatal frequency (McElwain et al., 2005).

Supplemental Figures

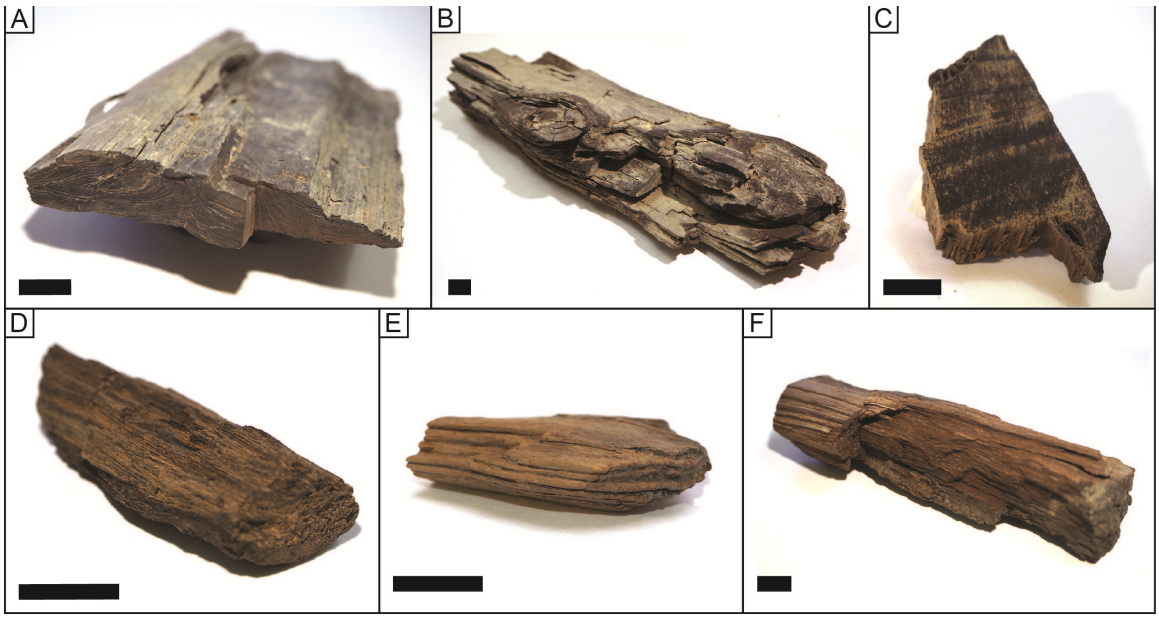

Figure DR1. Representative samples of deep-time mummified (non-permineralized) wood used in this study. All scale bars are 1 cm wide. A) Sample IC-02 from Early Eocene, Banks Island, Canada. Cellulose yield = 0.6%, ε = 2.7‰. Note very thin growth rings on front cross-section. Marks on recessed cross-sectional face are saw cut marks. B) Sample ER-05_02 from Early Eocene, Banks Island, Canada. Cellulose yield could not be calculated due to sediment admixed with extracted cellulose, ε = 3.1‰. Faint growth rings present. C) Sample NNW069 from Oligocene, Nanning, China. Cellulose yield = 44.5%, ε = 1.3‰. Note growth rings on roughly polished front cross-section. D) Sample NNW40 from Oligocene, Nanning, China. Cellulose yield = 1.7%, ε = 3.3‰. Thin growth rings are present. E) Sample FC13-04 from Miocene, Finish Stream, Russia. Cellulose yield = 18.9%, ε = 2.3‰. Thin growth rings are present. F) Sample NF01 from Miocene, Yunnan, China. Cellulose yield = 2.7% ε = 3.2‰. Growth rings present.

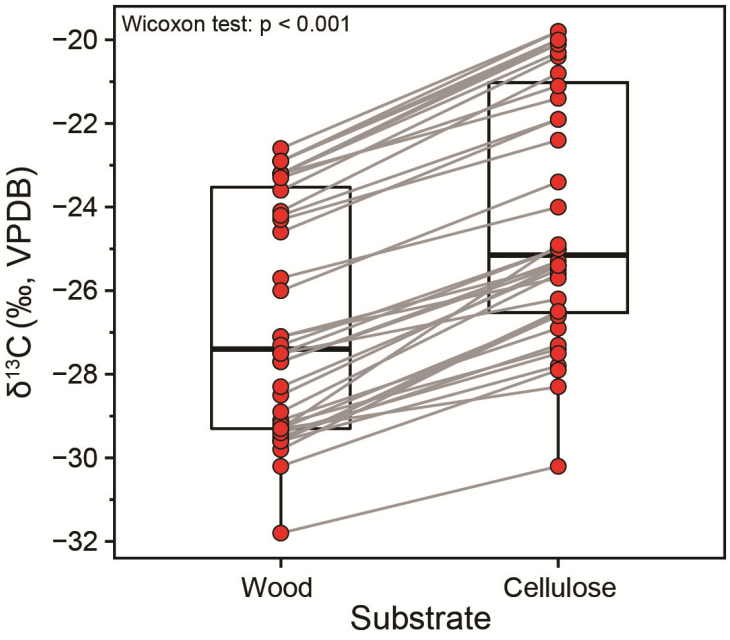

Figure DR2. Boxplots of deep-time $\delta^{13}C_{wood}$ and $\delta^{13}C_{cell}$ values, with lines connecting paired samples (n = 38). Boxes extend from the first to third quartile; bold crossbar indicates second quartile (median). Whiskers extend to 1.5 times the interquartile range (third quartile minus first quartile). The $\delta^{13}C_{wood}$ values are significantly lower than $\delta^{13}C_{cell}$ values (Wilcoxon test, p < 0.001); $\delta^{13}C_{cell}$ values are higher than $\delta^{13}C_{wood}$ in every pair (gray tie lines).

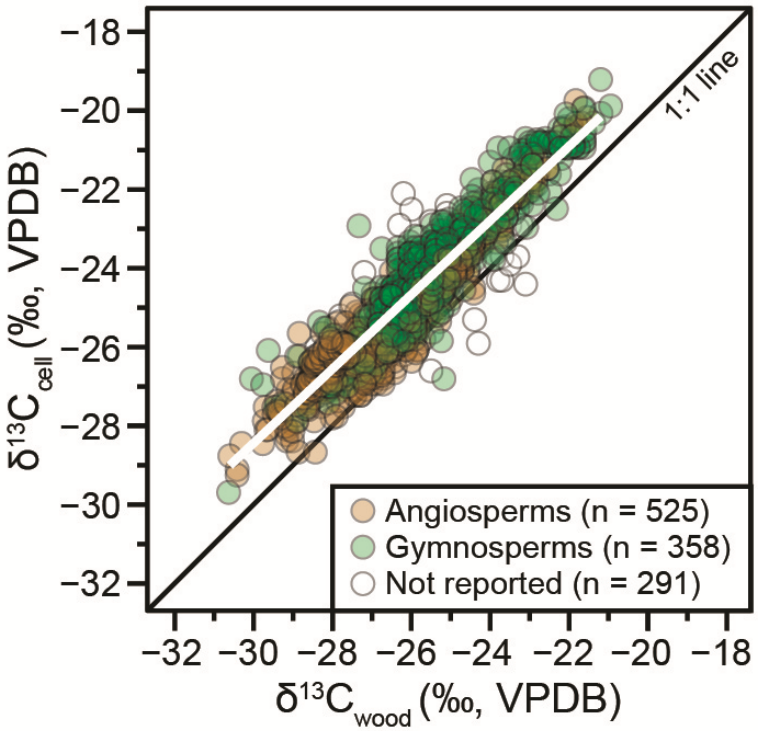

Figure DR3. Cross-plot of $\delta^{13}C_{cell}$ versus $\delta^{13}C_{wood}$ for all Holocene data (12 ka to present), coded by angiosperms and gymnosperms. Gymnosperms have significantly higher $\delta^{13}C_{cell}$ and $\delta^{13}C_{wood}$ values than angiosperms (Wilcoxon test, $p < 0.001$ for each). Deviation from the 1:1 line indicates apparent enrichment (ε) between $\delta^{13}C_{cell}$ and $\delta^{13}C_{wood}$. Regression line is for all samples shown.

Supplemental Tables

Table DR1
2019354_Table DR1.xlsx

Table DR2
2019354_Table DR2.xlsx

References

Brendel, O., Iannetta, P. P. M., and Stewart, D., 2000, A rapid and simple method to isolate pure α-cellulose: Phytochemical Analysis, v. 11, no. 1, p. 7-10.

Coplen, T. B., Brand, W. A., Gehre, M., Groning, M., Meijer, H. A. J., Toman, B., and Verkouteren, R. M., 2006, After two decades a second anchor for the VPDB delta C-13 scale: Rapid Communications in Mass Spectrometry, v. 20, no. 21, p. 3165-3166.

Dong, W., Upper Cenozoic stratigraphy and paleoenvironment of Xiaolongtan Basin, Kaiyuan, Yunnan Province, *in* Proceedings Proceedings of the Eighth Annual Meetings of Chinese Society of Vertebrate Paleontology2001, Volume 8.

Gaudinski, J. B., Dawson, T. E., Quideau, S., Schuur, E. A. G., Roden, J. S., Trumbore, S. E., Sandquist, D. R., Oh, S.-W., and Wasylishen, R. E., 2005, Comparative analysis of cellulose preparation techniques for use with ^{13}C, ^{14}C, and ^{18}O isotopic measurements: Analytical Chemistry, v. 77, no. 22, p. 7212-7224.

Hesselbo, S. P., Jenkyns, H. C., Duarte, L. V., and Oliveira, L. C. V., 2007, Carbon-isotope record of the Early Jurassic (Toarcian) Oceanic Anoxic Event from fossil wood and marine carbonate (Lusitanian Basin, Portugal): Earth and Planetary Science Letters, v. 253, no. 3–4, p. 455-470.

Huang, L., Jin, J., Quan, C., and Oskolski, A. A., 2018, Mummified fossil woods of Fagaceae from the upper Oligocene of Guangxi, South China: Journal of Asian Earth Sciences, v. 152, p. 39-51.

C. D. Keeling, S. C. Piper, R. B. Bacastow, M. Wahlen, T. P. Whorf, M. Heimann, and H. A. Meijer, 2001, Exchanges of atmospheric CO2 and 13CO2 with the terrestrial biosphere and oceans from 1978 to 2000: I. Global aspects, SIO Reference Series, No. 01-06, Scripps Institution of Oceanography, San Diego, 88 pages.

McElwain, J. C., Wade-Murphy, J., and Hesselbo, S. P., 2005, Changes in carbon dioxide during an oceanic anoxic event linked to intrusion into Gondwana coals: Nature, v. 435, no. 7041, p. 479-482.

Padilla, A., Eberle, J. J., Gottfried, M. D., Sweet, A. R., and Hutchison, J. H., 2014, A sand tiger shark–dominated fauna from the Eocene Arctic greenhouse: Journal of Vertebrate Paleontology, v. 34, no. 6, p. 1307-1316.

Prokoph, A., Shields, G. A., and Veizer, J., 2008, Compilation and time-series analysis of a marine carbonate $\delta^{18}O$, $\delta^{13}C$, $^{87}Sr/^{86}Sr$ and $\delta^{34}S$ database through Earth history: Earth-Science Reviews, v. 87, no. 3, p. 113-133.

Quan, C., Fu, Q., Shi, G., Liu, Y., Li, L., Liu, X., and Jin, J., 2016, First Oligocene mummified plant Lagerstätte at the low latitudes of East Asia: Science China Earth Sciences, v. 59, no. 3, p. 445-448.

Schubert, B. A., and Jahren, A. H., 2015, Global increase in plant carbon isotope fractionation following the Last Glacial Maximum caused by increase in atmospheric pCO_2: Geology v. 43, no. 5, p. 435-438.

Schubert, B. A., Jahren, A. H., Davydov, S. P., and Warny, S., 2017, The transitional climate of the late Miocene Arctic: Winter-dominated precipitation with high seasonal variability: Geology, v. 45, no. 447-450.

Schubert, B. A., Jahren, A. H., Eberle, J. J., Sternberg, L. S. L., and Eberth, D. A., 2012, A summertime rainy season in the Arctic forests of the Eocene: Geology, v. 40, no. 6, p. 523-526.

van Hinsbergen, D. J. J., de Groot, L. V., van Schaik, S. J., Spakman, W., Bijl, P. K., Sluijs, A., Langereis, C. G., and Brinkhuis, H., 2015, A paleolatitude calculator for paleoclimate studies (model version 2.0): PLOS ONE, v. 10, no. 6, p. e0126946.

Wang, X. R., Tsumura, Y., Yoshimaru, H., Nagasaka, K., and Szmidt, A. E., 1999, Phylogenetic relationships of Eurasian pines (Pinus, Pinaceae) based on chloroplast rbcL, matK, rpl20-rps18 spacer, and trnV intron sequences: American Journal of Botany, v. 86, no. 12, p. 1742-1753.

Xing, Y., Liu, Y.-S. C., Su, T., Jacques, F. M., and Zhou, Z., 2010, Pinus prekesiya sp. nov. from the upper Miocene of Yunnan, southwestern China and its biogeographical implications: Review of Palaeobotany and Palynology, v. 160, no. 1-2, p. 1-9.

Ying, T., Shaw, D., and Schneider, S., 2018, Oligocene fossil assemblages from Lake Nanning (Yongning Formation; Nanning Basin, Guangxi Province, SE China): Biodiversity and evolutionary implications: Palaeogeography, Palaeoclimatology, Palaeoecology, v. 505, p. 100-119.

Zhang, Y. P., 1974, Miocene suids from Kaiyuan, Yunnan and Linchu, Shantung: Vertebrata Palasiatica, v. 12, no. 2, p. 117-123.

Zhao, Z., 1993, New Anthracothere materials from the Paleogene of Guangxi: Vertebrata PalAsistica, v. 31, p. pl. 1.

Zhou, Z., 1985, The Miocene Xiaolongtan fossil flora in Kaiyuan, Yunnan, China, Nanjing Institute of Geology and Palaeontology, Chinese Academy of Sciences.

Zhou, Z. K., 2000, Miocene flora of Yunnan Province, *in* Tao, J. R., Zhou, Z. K., and Liu, Y. S., eds., The Evolution of the Late Cretaceous–Cenozoic Floras in China: Beijing, China, Science Press, p. 64-72.